

UWC: Unit-wise Calibration Towards Rapid Network Compression

Chen Lin¹

linchen7@hikvision.com

Zheyang Li¹²

lizheyang@hikvision.com

Bo Peng¹

pengbo7@hikvision.com

Haoji Hu²

haoji_hu@zju.edu.cn

Wenming Tan¹

tanwenming@hikvision.com

Ye Ren¹

renye@hikvision.com

Shiliang Pu¹

pushiliang@hikvision.com

¹ Hikvision Research Institute

Hangzhou, China

² Zhejiang University

Hangzhou, China

Abstract

This paper introduces a post-training quantization (PTQ) method achieving highly efficient Convolutional Neural Network (CNN) quantization with high performance. Previous PTQ methods usually reduce compression error via performing layer-by-layer parameters calibration. However, with lower representational ability of extremely compressed parameters (e.g., the bit-width goes less than 4), it is hard to eliminate all the layer-wise errors. This work addresses this issue via proposing a unit-wise feature reconstruction algorithm based on an observation of second order Taylor series expansion of the unit-wise error. It indicates that leveraging the interaction between adjacent layers' parameters could compensate layer-wise errors better. In this paper, we define several adjacent layers as a Basic-Unit, and present a unit-wise post-training algorithm which can minimize quantization error. This method achieves near-original accuracy on ImageNet and COCO when quantizing FP32 models to INT4 and INT3.

1 Introduction

Network compressions [10, 13, 15, 18, 28, 4, 30] are essential techniques when deploying Deep Neural Networks (DNNs) to edge devices such as smartphones or wearable devices. Recent compression works could be roughly divided into two categories: structure simplification and quantization. Structure simplification reduces the float point operations (FLOPs) and the memory footprint of DNNs by tensor factorization [8, 11], sparse connection [13], weight

pruning, neuron pruning, channel pruning [20, 21], etc. Among them, channel pruning is a simple but effective approach which is applied in various applications, it directly removes redundant connections and re-trains the pruned network structure. Quantization [24, 28, 30, 33] is another practical approach. It reduces the complexity of network by approximating full precision weights and activations to low-bit ones. In this paper, we investigate quantization to achieve extremely efficient implementations of CNNs.

To achieve guaranteed performance, the quantization users usually perform a Quantization-aware Training (QAT) [20, 21, 23, 25, 26] process. These approaches are not practical solutions in industry for at least two reasons. The long time re-training and requirements of full training data consumes unacceptable computation and storage resources, leading to a tedious deployment pipeline. Moreover, the requirements of full dataset may involve privacy issues. To avoid above issues, the PTQ methods [8, 12, 21, 24, 25] that efficiently turns float-point model to fixed-point counterpart with only a small calibration set, become prevalent in industry. PTQ is fast and light, while predominant approaches simply applying Rounding-to-nearest suffer performance degradation when the compression rate goes higher (e.g. the bit-width goes less than 4 bits).

To retain the accuracy, some layer-wise reconstruction-based algorithms (e.g. AdaRound [21], Bit-Split [23], AdaQuant [24]) are proposed. These methods greatly improve the 4-bit quantization accuracy because the layer-wise reconstruction loss **implicitly leverages the interaction between weights in each layer** to reduce the error incurred due to quantization. However, the parameters space of a single quantized layer is much smaller than the original layer's. When the compression rate goes higher, the layer-wise features in quantized network are not well-fitted to the original counterparts, leading to the accumulation of error through networks. Recently, BRECQ[16] proposes a block-wise reconstruction algorithm implicitly leveraging the cross-layer interaction in a block. Nevertheless, when quantizing compact models (e.g., MobileNet), it still remains a non-negligible gap in accuracy with original model. Since the weights in different blocks are never jointly optimized, the ignorance of some important cross-block interactions might hinder them to achieve higher accuracy. Different from Brecq [16], this paper divides the network into several overlapped units, which will not miss the interaction information between blocks.

In this paper, we formulate PTQ problem as follows. Given a calibration set with 128 to 1024 instances and a well-trained neural network, our algorithm is directed toward a twofold goal: (1) **In terms of performance**, the quantized model remains near original performance while weights are turned to lower than 4 bits. (2) **In terms of efficiency**, the whole process is expected to be quick enough to be applicable in production lines (e.g., within 30 minutes).

- To achieve goal (1), we theoretically analyze the impact on the task loss due to quantization based on a second series Taylor expansion. This analysis inspires us to explicitly extract the interaction matrix between adjacent layers to enhance the performance. Then, a unit-wise reconstruction objective embedded with above interaction is proposed to eliminate the quantization error.
- To achieve goal (2), we further propose an arguable two-stage search space simplification which makes the unit discrete space much smaller and differentiable to make the stochastic gradient descent (SGD) strategy feasible. After that, the complexity of unit-wise optimization is reduced to a reasonable range.

Experiments well demonstrate that our proposed unit-wise algorithm possesses not only high performance, but also great compression ratio. A near original model performance is achieved

even when quantizing FP32 models to INT3. The rest of this paper is organized as follows. Section 2 analyze current network compressions in quantization. The motivation and the proposed unit-wise optimizing algorithm is introduced in Section 3.1 and 3.2. Section 4 performs extensive experiments on several benchmarks with in-depth analysis.

2 Related Work

Standard implementation of DNNs is inefficient in memory storage and consumes considerable computational resources. Many network compression techniques tried to simplify and accelerate DNNs. Quantization is one of the most effective ways of saving the consumption of neural networks during inference by converting the high precision operations into lower precision ones. There are two main regimes of network quantization: Quantization-Aware Training and Post-Training Quantization.

Quantization-Aware Training. Previous works mainly insert quantization operation in the re-training process to retain high performance, which is called quantization-aware training (QAT). [1] uses a straight through estimator to pass through the gradients of quantization operations. After that, many methods extended these training frameworks, e.g. [2] trains parameterized clipping thresholds for quantized network. [3] uses a differentiable tanh function to gradually quantize the network. [4] learns the quantization interval as well as the bit-width per layer for mix-precision networks. Although QAT gains good performance, it usually costs long training times as well as numerous energy spent during network training.

Post-Training Quantization. Post-training quantization (PTQ) is a lightweight approach since it doesn't require the original training pipeline. ACIQ [5] fits Gaussian and Laplacian models to the distribution for optimal clip threshold. [6] leverages model expansion to improve quantization. [7] split the bits of weight to compensate quantization error. [8] optimizes the rounding operation to improve the final loss. BRECQ[16] proposes a block-wise reconstruction algorithm implicitly leveraging the cross-layer interaction in a block. In most cases, PTQ methods are sufficient for achieving near-original accuracy under 8-bit quantization, while the performance reduction becomes non-negligible when the bit-width goes less than 4-bit.

Notation. We use capital bold letters and small bold letters denoting matrices (or tensors) and vectors, respectively. For instance, \mathbf{W} and \mathbf{w} represent the weight tensor and its flatten version. All vectors are considered to be column vectors. The bracketed superscript and the subscript indicate the layer and the element indices, e.g., $\mathbf{W}_{a,b}^{(i)}$, $\mathbf{x}^{(i)}$. For deep neural network with L layers, we mark all the flattened parameters by \mathbf{w} , where $\mathbf{w} = \text{vec} \left[\mathbf{w}^{(1),T}, \dots, \mathbf{w}^{(i),T}, \dots, \mathbf{w}^{(L),T} \right]^T$ is the concatenation of all layers' weights. Quantization turns the weights $\mathbf{w} \in \mathbb{R}^d$ to discrete set $\hat{\mathbf{w}} \in \mathbb{V}^d$, where $\mathbb{V} = \alpha \times \{-2^{b-1}, \dots, 2^{b-1} - 1\}$ is the potential value space of each element, b is the bit width and α is the interval of quantization.

3 Method

In this section, we will introduce our proposed approach centered around performance and efficiency. In Section 3.1, we propose a Unit-wise Objective embedded with an interaction

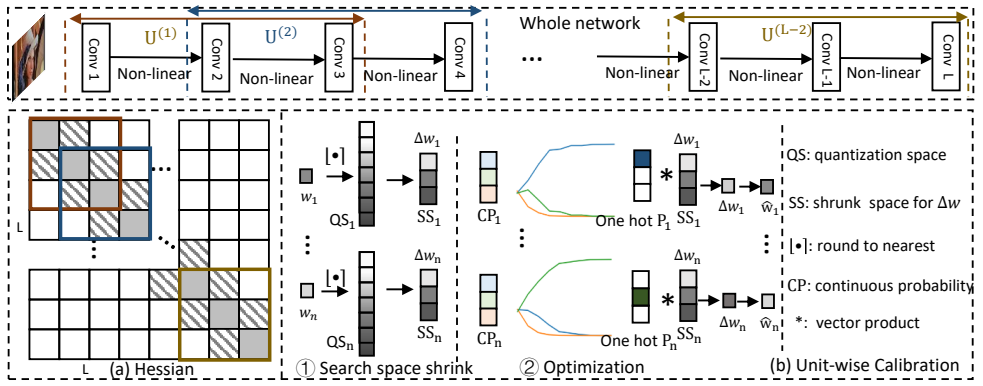


Figure 1: **Overview of the proposed approach.** The whole network is divided into several basic optimizing units. For each unit, a unit-wise optimizing algorithm is applied. (a) shows the whole Hessian H of an L -layer network. Ignoring the interaction between layers that are non-adjacent, H becomes block tridiagonal matrix. Defining three connected layers as a basic unit, the L -layer network is divided into $L - 2$ units, $u^{(1)}, u^{(2)}, \dots, u^{(L-2)}$. The circled squares are the corresponding Hessian of these units. (b) shows a two stage two-stage search space simplification. In ① search space shrink, each quantized weight \hat{w}_i is suggested to select one of the three quantization grids that are near the original weight w_i . The size of Δw_i 's search space SS_i is shrunk to 3. In ② Optimization, the probability over SS_i is first relaxed to continuous values CP_i , and then gradually pushed to a one-hot vector P_i . After optimization, the optimal value of \hat{w}_i is selected.

matrix to enhance quantization performance. In Section 3.2, an efficient optimization strategy is introduced based on a two-stage search space simplification.

3.1 Unit-wise Objective

Let's begin with analyzing the increase in task loss \mathcal{L} (e.g., cross-entropy loss for classification) introduced by quantization. Quantization turns float-point weight w to fixed-point weight \hat{w} , which inevitably adds a perturbation $\Delta w = \hat{w} - w$ on w . The expected increase in task loss w.r.t. Δw can be approximated by the second order Taylor series expansion

$$\begin{aligned} \mathbb{E}[\Delta \mathcal{L}(\Delta \mathbf{w})] &= \mathbb{E}(\mathcal{L}(\Delta \mathbf{w} + \mathbf{w}, \mathbf{x}, \mathbf{y}) - \mathcal{L}(\mathbf{w}, \mathbf{x}, \mathbf{y})) \\ &\approx \Delta \mathbf{w}^T g(\mathbf{w}) + \frac{1}{2} \Delta \mathbf{w}^T H(\mathbf{w}) \Delta \mathbf{w}, \end{aligned} \quad (1)$$

where \mathbb{E} is the expectation operator, $g(\mathbf{w})$ and $H(\mathbf{w})$ are the expected gradient and Hessian of \mathcal{L} w.r.t. $\Delta \mathbf{w}$. The first order term vanishes as the model converged to local minimal, i.e., $g(\mathbf{w})$ is close to zero.

Eq. (1) implies that different perturbed weights are interactive in terms of the task loss, and $H(\mathbf{w})$ defines the interaction. For example, consider two elements $[w_i, w_j]$ in \mathbf{w} , and the hessian matrix of \mathcal{L} w.r.t. $[w_i, w_j]$ is $\begin{bmatrix} H_{i,i} & H_{i,j} \\ H_{j,i} & H_{j,j} \end{bmatrix} = \begin{bmatrix} 1 & 0.5 \\ 0.5 & 1 \end{bmatrix}$. Assume we only quantized w_i and $\Delta w_i = 1$, then its introduced increase in loss is $\Delta \mathcal{L}_{(\Delta w_1=1, \Delta w_2=0)} = H_{i,i} \Delta w_i = 1$. By using the joint impact of $[\Delta w_1, \Delta w_2]$ on the loss $\Delta \mathcal{L}_{(\Delta w_1=1, \Delta w_2)} = (\Delta w_2)^2 + \Delta w_2 + 1$, we can reduce the error due to Δw_1 by adjusting Δw_2 , i.e., when $\Delta w_2 = -0.5$, the loss is reduced

to 0.75. This simple case inspires us that the quantization error can well be reduced if the interaction of all weights are jointly considered. Therefore, we reformulate minimizing the second order term as our objective,

$$\underset{\Delta \mathbf{w}}{\text{minimize}} \quad \Delta \mathbf{w}^T H(\mathbf{w}) \Delta \mathbf{w}. \quad (2)$$

(2) is a good proxy as it overall reduces the joint impact on the task loss of all the perturbed weights. However, it is not tractable to directly optimize (2) because of the storage and computation budget. For a network with n parameters (potentially millions of parameters), $O(n^2)$ footprint is needed to store the Hessian and $O(n^3)$ computations are needed for each optimization step.

Above analysis motivates us to leverage the interaction between weights to enhance quantization. In the following, we will capture the main information of $H(\mathbf{w})$ with some approximations to constraints the complexity to a reasonable range. As the weight \mathbf{w} is the concatenation of all layers' weights, $H(\mathbf{w}) = E\left(\frac{\partial^2 \mathcal{L}}{\partial \mathbf{w}^2}\right)$ can be viewed as a L by L block matrix, with the (i, j) -th block $H^{(i,j)}$ given by $H^{(i,j)} = E\left(\frac{\partial^2 \mathcal{L}}{\partial \mathbf{w}^i \partial \mathbf{w}^j}\right)$. And $H^{(i,j)}$ represents the interaction between layer i and layer j .

As shown in Figure 1 (a), adjacent layers are higher interactive while non-adjacent layers are lower interactive. This is explainable as computing $\mathbf{g}^{(i)}$ only directly uses the input information from layer $i - 1$ and the gradient information from layer $i + 1$. To reduce the budget, it is reasonable to ignore the interaction between weights of non-adjacent layers. Therefore, assuming $|j - i| > \delta$, $H^{(i,j)} = 0$, a fragment of u connected layers are considered interactive, where $u = 2\delta + 1$. After that, as shown in Figure 1 (c), the Hessian H become a block tridiagonal matrix. This motivates us to divide the model into multiple overlapped units and optimize each unit sequentially.

Formally, we define u adjacent layers as a basic optimization unit $\text{vec}[\mathbf{w}^{(i),T}, \dots, \mathbf{w}^{(i+u),T}]$. The overall objective Eq. (2) is then transformed to a set of unit-wise objectives. For i -th unit, the unit-wise objective is formulated as

$$\underset{\Delta \mathbf{W}^{(i)}, \dots, \Delta \mathbf{W}^{(i+u)}}{\text{minimize}} \sum_{k=0, j=0}^{u, u} \Delta \mathbf{w}^{(i+k),T} H^{(i+k, i+j)} \Delta \mathbf{w}^{(i+j)}. \quad (3)$$

Although Eq. (3) greatly speed up Eq. (2) by the tridiagonal approximation of H , optimizing Eq. (3) is still infeasible for the budget associated with block entry $H^{(i+k, i+j)}$.

In the following, we will further simplify Eq. (3). To avoid repeatedly calculating each block entry $H^{(i+k, i+j)}$ (see [15]), we first reformulate Eq.(3) to make all block entries related to the pre-activation Hessian $\mathcal{H}^{(i+u)}$ (see [16]),

$$\sum_{k=0, j=0}^{u, u} \Delta \mathbf{w}^{(i+k),T} J \left[\frac{\mathbf{z}^{(i+u)}}{\mathbf{w}^{(i+k)}} \right]^T \mathcal{H}^{(i+u)} J \left[\frac{\mathbf{z}^{(i+u)}}{\mathbf{w}^{(i+k)}} \right] \Delta \mathbf{w}^{(i+j)}, \quad (4)$$

where $\mathbf{z}^{(i+u)}$ is the pre-activation of layer $i + u$, given by $\mathbf{z}^{(i+u)} = \mathbf{W}^{(i)} \mathbf{x}^{(i+u-1)}$, $\mathcal{H}^{(i+u)}$ is the Hessian of \mathcal{L} w.r.t. $\mathbf{z}^{(i+u)}$, $J \left[\frac{\mathbf{x}}{\mathbf{y}} \right]$ is the expected Jacobian matrix of \mathbf{x} w.r.t. \mathbf{y} . When optimizing weights in a unit, we assume that elements in the unit outputs are not interactive, that is, $\mathcal{H}^{(i+u)}$ is diagonal. This assumption will not bring in large performance drop since the units are overlapped. The interaction between the unit outputs will be considered when optimizing

the next unit. We end up with the following objective

$$\underset{\Delta \mathbf{w}^{(i)}, \dots, \Delta \mathbf{w}^{(i+u)}}{\text{minimize}} \sum_{k=0}^u \left\| \sqrt{\text{diag}(\mathcal{H}^{(i+u)})} \mathbf{J} \left[\frac{\mathbf{z}^{(i+u)}}{\mathbf{w}^{(i+k)}} \right] \Delta \mathbf{w}^{(i+k)} \right\|_F, \quad (5)$$

where $\|\cdot\|_F$ is Frobenius norm. In Eq. (5), $\mathbf{M}^k = \sqrt{\text{diag}(\mathcal{H}^{(i+u)})} \mathbf{J} \left[\frac{\mathbf{z}^{(i+u)}}{\mathbf{w}^{(i+k)}} \right]$ is the captured interaction between weights in a unit. $\mathbf{J} \left[\frac{\mathbf{z}^{(i+u)}}{\mathbf{w}^{(i+k)}} \right] = \mathbb{E} \left[\mathbf{x}^{(i+k-1),T} \prod_k^u B^{(i+k)} \mathbf{W}^{(i+k)} \right]$ (see [19]), where $B^{(i+k)} = \text{diag}(\phi(\mathbf{z}^{(i+k)})')$ is the gradient of activation function. Here, we introduce some details in algorithm implementation. To avoid the second derivative, $\text{diag}(\mathcal{H}^{(i+u)})$ can be replaced by the diagonal Fisher Information matrix, that is, $\sqrt{\text{diag}(\mathcal{H}^{(i+u)})} \approx \frac{\partial \mathcal{L}}{\partial z^{(i+u)}}$, which is proven effective in [16] and [26].

Optimizing (5) does not suffer from complexity issue associated with H . The unit-wise optimization is still the least square regression problem with discrete constraints. The search space scales exponentially in the dimension of unit weights.

3.2 Unit-wise Calibration

Note that there are $2^b - 1$ possible values for each element, the combined solution space size is $(2^b - 1)^{n^u}$, where n^u is the numbers of elements in the unit. It is not efficient to make exhaustive search. Meanwhile, the widely used Straight Through Estimator (STE) [5] is not effective in this case for the inaccurate gradients. To reduce the complexity of optimization without performance degradation, we propose a two-stage search space simplification as follows.

Search space shrink. Before optimization, we first initialize each quantized weight $\widehat{w}_{\text{init}}$ to its nearest quantization grid by applying round-to-nearest on w . The absolute value of perturbation $\Delta \widehat{w}_{\text{init}}$ for each weight is smaller than $\frac{1}{2}\alpha$, where $\Delta \widehat{w}_{\text{init}} = w - \widehat{w}_{\text{init}}$, α a floating-point scale factor, representing the quantization interval. α for each weight is calculated and used like previous low-bit quantization method [1]. Since the added perturbations for all weights in a unit are small values, we suggest that the optimal $\Delta \widehat{w}$ will be selected around $\Delta \widehat{w}_{\text{init}}$. Such that, we shrink the search space of $\Delta \widehat{w}$ to $\mathbb{V} = \{-\alpha + \Delta \widehat{w}_{\text{init}}, \Delta \widehat{w}_{\text{init}}, \alpha + \Delta \widehat{w}_{\text{init}}\}$. The solution space size is shrunk to 3^{n^u} .

Optimization. With a much smaller search space, we have to tackle the inaccurate gradient estimation problem of STE in discrete set. Inspired by [33], we relax discrete $\Delta \mathbf{w}$ to continuous value space and gradually push the solution into discrete space \mathbb{V} during optimization process. For each element Δw in a unit, an auxiliary vector $\mathbf{a} \in \mathbb{R}^m$ is created to learn the distribution P of Δw , where m is the size of search space \mathbb{V} , here, $m = 3$. The probability P_i for selecting i -th element in \mathbb{V} is computed by

$$P_i = \frac{\exp^{\mathbf{a}_i/t}}{\sum_j \exp^{\mathbf{a}_j/t}}, \quad (6)$$

where t is a temperature factor designed to implicitly work as a regularizer. When t approaches to zero, P_i will converge to 0 or 1. During optimizing, Δw is displaced by a continuous expectation of Δw_e , and is calculated according to the probability over all the discrete values:

$$\Delta w_e = \sum_i V_i P_i, \quad (7)$$

Both Eq. (6) and Eq. (7) are differentiable thus gradients will be accurately estimated. SGD is applied on \mathbf{a} to adjust the distribution of Δw . By gradually decreasing the temperature t , the distribution P will be pushed to one-hot vector.

3.3 Discussion

Although our work shares a general form of optimizing multiple layers with BRECQ[[16](#)], our work is actually starkly different from theirs in many axes:

Motivation. Our method is always driven by the motivation, that is, fully making use of the whole network interaction (the Hessian) to reduce quantization error. Due to the intractability caused by the large Hessian, our method is developed to a set of overlapped unit-wise objectives to extract the main information from the whole Hessian. Different from ours, BRECQ is motivated to use the local Hessians from parts of the network. Their method is designed to choose an optimal reconstruction granularity from 4 kinds of granularity, i.e., layer, block, stage, network.

Basis of optimizing granularity. The optimizing granularity of our method comes from the assessment of interaction degree while their choice of block-wise optimization comes from experiments. Each unit, in our method, jointly optimizes multiple layers which have strong interaction, theoretically a sub-matrix with big values from the Hessian. This work sets three adjacent layers, i.e., the most interactive, as a unit for keeping the implementation simple to demonstrate the effectiveness of the interaction. Actually, our work can be extended to figure out optimal units dividing strategy by cropping sub-matrices with bigger values in the Hessian without constraints of layer numbers.

The approximation of the network Hessian. In our paper, the Hessian is simplified as a tri-diagonal block matrix while BRECQ's is diagonal block. Since the blocks are overlapped in our method, the interaction of adjacent optimization units is added comparing with BRECQ. The ignorance of some important cross-unit interactions might hinder them to achieve higher accuracy.

Empirical performance. Results show our method outperforms BRECQ's on ImageNet which may mainly benefit from the addition of cross-unit interaction.

4 Experiments

In this section, we evaluate the effectiveness of our proposed method on various computer vision tasks and models. Section 4.1 presents ablation study on the unit-wise optimization. In Section 4.2, we compare unit-wise with other post-training quantization methods. In Section 4.2, we present the performance of unit-wise calibration on object detection and instance segmentation tasks.

Experimental setup. For all experiments we absorb batch normalization into the weights of its previous connected convolutional layer. For all networks, the first layer and the last layer are quantized to 8-bit. We apply symmetric per-channel quantization for weights and symmetric per-tensor quantization for activations, which is a general and hardware-friendly development mode. For all experiments, we sample images from the training dataset as a calibration set. In optimization, the calibration data are cropped and resized into 224×224 , except for the InceptionV3 model whose input size is 299×299 , which is same as the training pipeline. We sequentially feed all the calibration data to the networks with the batch-size of 128. All optimizing and testing codes are built on Pytorch [[22](#)].

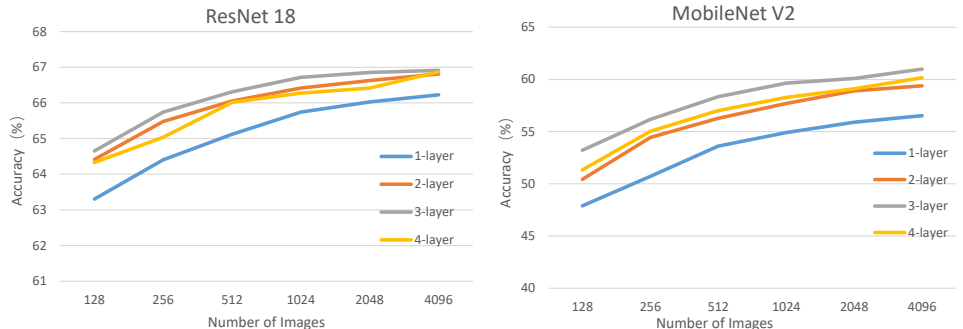


Figure 2: The effect on ImageNet validation accuracy when setting different numbers of layers for each unit under various data limitation.

4.1 Ablation Study

First, we determine the optimal number of layers for each unit and the size of calibration data. Limiting the number of calibration data in the range from 128 to 4096, we quantize the weights of ResNet18 and MobileNetV2 to 2-bit on ImageNet. To make sure the algorithm accomplishes within 30 minutes (0.5 GPU hours), we optimize each unit 20000 rounds. Figure 2 shows that when a unit contains 3 layers, the models outperform other options under various data limitations. The possible reason for this phenomenon is, for a layer i , the most interactive layers are the directly connected layer below (layer $i - 1$) and layer above (layer $i + 1$). When the number of layers goes up to 4, more calibration data and optimization rounds might be required for better performance. In the following experiments, we will set 3 layers for each unit and set the number of calibration data to 1024.

Layer-wise vs Unit-wise. We investigate the benefits of our proposed unit-wise optimization algorithm by comparing with layer-wise optimization algorithm. In our experiments, five widely used convolutional models, including Resnet18, Resnet50, Resnet101 [10], InceptionV3 [11], MobileNetV2 [12] and MobileNetV3 large [13] are used for comparison. All the pre-trained models are trained on ImageNet [14] and loaded from torchvision. As a baseline, we also perform a Layer-wise optimization to validate the effectiveness of cross-layer interaction,

Table 1: Comparison with Layer-wise reconstruction on ImageNet classification benchmark. Top-1 and Top-5 accuracy (%) are reported. Post-training quantization are conducted on weights and activations. Weights are quantized to 3 or 4 bits. Activations are quantized to 4/8 bits or remain un-quantized for comparison. **Bold values** indicates best results.

Algorithms	Bits(W/A)	Resnet18		Resnet50		Resnet101		InceptionV3		MobileNetV2		MobileV3-large	
		Top-1	Top-5	Top-1	Top-5								
FP.	32/32	69.76	89.08	76.25	92.88	77.57	93.76	77.57	93.69	71.88	90.29	74.04	91.34
Layer-wise	4/32	69.09	88.65	75.34	92.22	76.13	92.86	76.23	92.34	64.34	83.35	67.84	87.40
Unit-wise	4/32	69.43	88.76	75.83	92.62	77.13	93.54	76.88	92.82	71.17	89.33	72.26	89.91
Layer-wise	4/8	69.01	88.55	75.17	92.08	76.08	92.75	76.10	92.24	64.03	82.92	67.52	87.43
Unit-wise	4/8	69.44	88.81	75.77	92.44	77.21	93.41	76.48	92.75	70.89	89.31	72.02	89.77
Layer-wise	3/32	66.12	86.87	74.68	91.82	74.88	92.28	73.85	90.10	55.81	73.12	58.65	80.31
Unit-wise	3/32	68.72	88.49	74.97	92.23	76.24	92.22	75.93	92.82	69.42	88.23	68.72	86.71
Layer-wise	3/8	66.08	86.82	74.51	91.75	74.67	92.05	73.58	89.88	53.94	72.73	58.01	80.22
Unit-wise	3/8	68.42	88.09	74.54	92.00	75.98	92.22	75.71	92.48	68.92	87.52	67.32	85.62
Layer-wise	4/4	65.16	86.11	71.93	90.31	72.75	90.04	72.17	90.74	60.75	80.19	49.49	73.94
Unit-wise	4/4	67.23	87.13	74.38	91.67	75.74	92.08	74.44	91.95	64.78	83.76	64.97	83.69

Table 2: Comparison with State-of-the-arts post-training quantization approaches on ImageNet classification benchmark. Top-1 and Top-5 accuracy (%) are reported. **Bold** values indicate best results (with the least accuracy drop). \ddagger denotes the float point baselines of Brecq are different from ours (see first two rows in table). Weights are quantized to 3 or 4 bits and activations are remained un-quantized. * denotes quantizing our baseline models by the public released codes with our quantization space.

Algorithms	W/A	Resnet18		Resnet50		Resnet101		InceptionV3		MobilenetV2	
		Top-1	Top-5	Top-1	Top-5	Top-1	Top-5	Top-1	Top-5	Top-1	Top-5
FP.	32/32	69.76	89.08	76.25	92.88	77.57	93.76	77.57	93.69	71.88	90.29
FP(Brecq)	32/32	71.08	-	77.00	-	-	-	-	-	72.49	-
Bit-split [23]	4/32	69.11	88.69	75.58	92.57	76.89	93.31	-	-	-	-
AdaRound [24]	4/32	68.71	-	75.23	-	-	-	75.76	-	69.78	-
Brecq [16] \ddagger	4/32	70.70	-	76.29	-	-	-	-	-	71.66	-
Brecq [16]*	4/32	69.29	88.55	75.74	92.52	-	-	-	-	-	-
Ours	4/32	69.43	88.76	75.83	92.67	77.13	93.54	76.88	92.82	71.17	89.33
Bit-split [23]	3/32	66.76	87.45	73.64	91.61	74.98	92.42	-	-	-	-
AdaRound [24]	3/32	68.07	-	73.42	-	-	-	-	-	64.33	-
Brecq [16] \ddagger	3/32	69.81	-	75.61	-	-	-	-	-	69.50	-
Brecq [16]*	3/32	68.39	88.31	74.54	92.07	-	-	-	-	-	-
Ours	3/32	68.72	88.49	74.97	92.23	76.24	92.22	75.93	92.82	69.42	88.23
Brecq [16] \ddagger	2/32	66.30	-	72.40	-	-	-	-	-	59.67	-
Brecq [16]*	2/32	66.02	86.63	71.14	89.79	-	-	-	-	-	-
Ours	2/32	66.85	87.21	72.26	90.23	70.95	89.55	69.77	89.44	58.28	82.16

on these models. The results are shown in Table 1.

Shown in Table 1, the proposed unit-wise calibration method induces negligible accuracy degradation on all models even on the less redundant models, e.g. MobilenetV2. Under 4 bit quantization of weights, our quantized networks only induce 0.4% to 1.2% Top-1 accuracy drop on various networks. For the more aggressive 3 bit quantization of weights, our quantized networks only induce 0.5% to 1.7% Top-1 accuracy drop on most networks except MobilenetV2. In Table 1, we also report the results when activations are quantized to 8 bits and remained un-quantized, respectively. It is observed that 8 bits quantization for activations will lead to negligible performance degradation on all models.

Besides, unit-wise method outperforms the layer-wise method on all models. Especially on the comparison of 3 bits quantization of weights, the accuracy drop from layer-wise method is much larger. Another phenomenon is that the gap becomes larger when the original model becomes more compact, e.g. To evaluate the effectiveness on dynamic blocks implemented with SE, we conduct our algorithm on mobilenetv3-large model on ImageNet loaded from torchvision. In this experiment, each unit contains three adjacent layers not counting the layers in SEs since a SE module only takes a small amount of calculation and produces several scaling factors on features. The results show the superiority of unit-wise optimization.

We also evaluate our method under high compression rate for both weight and activation. The scale factors of activation quantizers are optimized using PACT in each unit. Shown in Table 1, when both activation and weights are quantized to 4-bit, unit-wise still outperforms layer-wise optimization.

4.2 Comparison with State-of-the-arts

Here, we evaluate our algorithm and compare with the State-of-the-arts post-training quantization approaches, including Bit-split [23], AdaRound [24] and Brecq [16]. Bit-Split splits the multiple-bits quantization optimization problem into multiple ternary quantization sub-

optimizations. After all the sub-optimizations, they stitch the multiple-bits into integers. AdaRound optimizes the rounding-to-nearest operations to reconstruct the final loss. Both Bit-Split and AdaRound fall into the layer-wsie reconstruction. Brecq proposes to choose block as a base reconstruction unit. In all approaches, weights are quantized to 3 or 4 bits, and activations are remained un-quantized. The results are shown in Table 2.

ImageNet Classification. Shown in Table 2, the proposed unit-wise calibration method outperforms all competing methods for both 3 and 4 bits. Under 4 bit quantization of weights, the compared methods still report good performance on the relatively redundant models, e.g., Resnets. However, for the more challenging networks, InceptionV3 and MobilenetV2, 4 bits quantization has a bigger impact. In this case, our method shows prominent superiority comparing with Bit-split and AdaRound. When the bit of weight goes down to 3, Bit-split and AdaRound result in more obvious performance degradation. Brecq achieves better results than Bit-split and AdaRound, while still has larger accuracy drop than ours especially on MobilenetV2. Our method outperforms Brecq since the cross-block interaction information are considered. For Resnets, our method leads to the smallest accuracy drop within 1.3%. For MobilenetV2, all other methods lead to un-tolerable performance degradation, while our approach obtain the best result with only 2.46% drop in accuracy. In the more aggressive 2-bit weights quantization, both ours and brecq’s show obvious loss of performance. However, the increase of cross-block interaction helps us get higher accuracy.

Object Detection and Instance Segmentation. To validate the effectiveness and applicability of unit-wise calibration, the experiments of object detection and instance segmentation tasks are applied. Unit-wise calibration has been evaluated on object detection with one-stage RetinaNet [10] and two-stage Faster R-CNN [25], Mask R-CNN [8], models. Also we evaluate it on instance segmentation with Mask R-CNN model. For all networks, we choose Resnet50 as backbone. MS COCO is adopted as the testing set to evaluate our method. For calibration and validation data, we resize them to 1333×800 . Since the input images are much bigger than classification images, only 400 images are sampled as calibration data. The bounding box AP for object detection and mask AP for instance segmentation are reported in Table 3. According to Table 3, we can see that there are about 0.4% to 0.9% mAP degradation without re-training the network, which demonstrate our method nearly achieves near-to-original performance with 4-bit weight and 8-bit activation quantization.

Table 3: Object Detection and Instance Segmentation performance on COCO val set. The first three lines report bounding box AP for object detection, and the last line reports mask AP for instance segmentation.

Model	Full Precision	A8W4
Faster R-CNN[25]	36.6	36.2
RetinaNet [10]	36.2	35.3
Mask R-CNN[8]	36.6	35.8
Mask R-CNN[9]	33.9	33.2

5 Conclusions

In this paper, we proposed a unit-wise post-training quantization algorithm. To improve the performance, the interaction between adjacent layers is extracted to eliminate quantization error. To speed up the optimization, a two-stage search space simplification is also proposed. The algorithm achieves near original accuracy using only 1024 samples within 0.5 GPU hours when weights are quantized to INT3 on tasks of ImageNet and COCO.

References

- [1] R. Banner, Yury Nahshan, E. Hoffer, and Daniel Soudry. Aciq: Analytical clipping for integer quantization of neural networks. *ArXiv*, abs/1810.05723, 2018.
- [2] Yoshua Bengio, Nicholas Léonard, and Aaron Courville. Estimating or propagating gradients through stochastic neurons for conditional computation, 2013.
- [3] Yaohui Cai, Zhewei Yao, Zhen Dong, Amir Gholami, Michael W. Mahoney, and Kurt Keutzer. Zeroq: A novel zero shot quantization framework, 2020.
- [4] Jungwook Choi, Zhuo Wang, Swagath Venkataramani, Pierce I-Jen Chuang, Vijayalakshmi Srinivasan, and Kailash Gopalakrishnan. Pact: Parameterized clipping activation for quantized neural networks, 2018.
- [5] Matthieu Courbariaux, Yoshua Bengio, and Jean-Pierre David. Binaryconnect: Training deep neural networks with binary weights during propagations, 2016.
- [6] J. Deng, W. Dong, R. Socher, L.-J. Li, K. Li, and L. Fei-Fei. Imagenet: A large-scale hierarchical image database. In *CVPR09*, 2009.
- [7] Ruihao Gong, Xianglong Liu, Shenghu Jiang, Tianxiang Li, Peng Hu, Jiazen Lin, Fengwei Yu, and Junjie Yan. Differentiable soft quantization: Bridging full-precision and low-bit neural networks, 2019.
- [8] Kaiming He, Xiangyu Zhang, Shaoqing Ren, and Jian Sun. Deep residual learning for image recognition. In *Proceedings of the IEEE conference on computer vision and pattern recognition*, pages 770–778, 2016.
- [9] Kaiming He, Georgia Gkioxari, Piotr Dollár, and Ross Girshick. Mask r-cnn, 2018.
- [10] Yihui He, Xiangyu Zhang, and Jian Sun. Channel pruning for accelerating very deep neural networks. In *Proceedings of the IEEE ICCV*, pages 1389–1397, 2017.
- [11] Andrew G Howard, Menglong Zhu, Bo Chen, Dmitry Kalenichenko, Weijun Wang, Tobias Weyand, Marco Andreetto, and Hartwig Adam. Mobilenets: Efficient convolutional neural networks for mobile vision applications. *arXiv preprint arXiv:1704.04861*, 2017.
- [12] Andrew G. Howard, M. Sandler, Grace Chu, Liang-Chieh Chen, B. Chen, Mingxing Tan, Weijun Wang, Yukun Zhu, Ruoming Pang, Vijay Vasudevan, Quoc V. Le, and Hartwig Adam. Searching for mobilenetv3. *2019 IEEE/CVF International Conference on Computer Vision (ICCV)*, pages 1314–1324, 2019.
- [13] Zehao Huang and Naiyan Wang. Data-driven sparse structure selection for deep neural networks. In *Proceedings of the European conference on computer vision (ECCV)*, pages 304–320, 2018.
- [14] Itay Hubara, Yury Nahshan, Yair Hanani, Ron Banner, and Daniel Soudry. Improving post training neural quantization: Layer-wise calibration and integer programming, 2020.
- [15] Hao Li, Asim Kadav, Igor Durdanovic, Hanan Samet, and Hans Peter Graf. Pruning filters for efficient convnets. *arXiv preprint arXiv:1608.08710*, 2016.

- [16] Yuhang Li, Ruihao Gong, Xu Tan, Yang Yang, Peng Hu, Qi Zhang, Fengwei Yu, Wei Wang, and Shi Gu. Brecq: Pushing the limit of post-training quantization by block reconstruction. *arXiv preprint arXiv:2102.05426*, 2021.
- [17] Tsung-Yi Lin, Priya Goyal, Ross Girshick, and Kaiming He. Focal loss for dense object detection. 2017.
- [18] Jian-Hao Luo, Jianxin Wu, and Weiyao Lin. Thinet: A filter level pruning method for deep neural network compression. In *Proceedings of the IEEE International Conference on Computer Vision (ICCV)*, Oct 2017.
- [19] James Martens and Roger Grosse. Optimizing neural networks with kronecker-factored approximate curvature. In *International conference on machine learning*, pages 2408–2417. PMLR, 2015.
- [20] Eldad Meller, Alexander Finkelstein, Uri Almog, and Mark Grobman. Same, same but different - recovering neural network quantization error through weight factorization, 2019.
- [21] Markus Nagel, Rana Ali Amjad, Mart van Baalen, Christos Louizos, and Tijmen Blankevoort. Up or down? adaptive rounding for post-training quantization, 2020.
- [22] Adam Paszke, Sam Gross, Francisco Massa, Adam Lerer, James Bradbury, Gregory Chanan, Trevor Killeen, Zeming Lin, Natalia Gimelshein, Luca Antiga, et al. Pytorch: An imperative style, high-performance deep learning library. In *Advances in neural information processing systems*, pages 8026–8037, 2019.
- [23] Wang Peisong, Qiang Chen, Xiangyu He, and Cheng Jian. Towards accurate post-training network quantization via bit-split and stitching. In *Proceedings of the 37nd International Conference on Machine Learning (ICML)*, pages 243–252, July 2020.
- [24] Mohammad Rastegari, Vicente Ordonez, Joseph Redmon, and Ali Farhadi. Xnor-net: Imagenet classification using binary convolutional neural networks. In *European conference on computer vision*, pages 525–542. Springer, 2016.
- [25] Shaoqing Ren, Kaiming He, Ross Girshick, and Jian Sun. Faster r-cnn: towards real-time object detection with region proposal networks. 2015.
- [26] Sidak Pal Singh and Dan Alistarh. Woodfisher: Efficient second-order approximations for model compression. *ArXiv*, abs/2004.14340, 2020.
- [27] Christian Szegedy, Vincent Vanhoucke, Sergey Ioffe, Jonathon Shlens, and Zbigniew Wojna. Rethinking the inception architecture for computer vision, 2015.
- [28] Stefan Uhlich, Lukas Mauch, Fabien Cardinaux, Kazuki Yoshiyama, Javier Alonso Garcia, Stephen Tiedemann, Thomas Kemp, and Akira Nakamura. Mixed precision dnns: All you need is a good parametrization, 2020.
- [29] Karen Ullrich, Edward Meeds, and Max Welling. Soft weight-sharing for neural network compression. *arXiv preprint arXiv:1702.04008*, 2017.

- [30] Kuan Wang, Zhijian Liu, Yujun Lin, Ji Lin, and Song Han. Haq: Hardware-aware automated quantization with mixed precision. In *Proceedings of the IEEE conference on computer vision and pattern recognition*, pages 8612–8620, 2019.
- [31] Peisong Wang and Jian Cheng. Fixed-point factorized networks. In *Proceedings of the IEEE Conference on Computer Vision and Pattern Recognition*, pages 4012–4020, 2017.
- [32] Peisong Wang, Qinghao Hu, Yifan Zhang, Chunjie Zhang, Yang Liu, and Jian Cheng. Two-step quantization for low-bit neural networks. In *Proceedings of the IEEE Conference on computer vision and pattern recognition*, pages 4376–4384, 2018.
- [33] Zhaohui Yang, Yunhe Wang, Kai Han, Chunjing Xu, Chao Xu, Dacheng Tao, and Chang Xu. Searching for low-bit weights in quantized neural networks, 2020.
- [34] Ritchie Zhao, Yuwei Hu, Jordan Dotzel, Christopher De Sa, and Zhiru Zhang. Improving neural network quantization without retraining using outlier channel splitting. In *ICML*, 2019.
- [35] Shuchang Zhou, Yuxin Wu, Zekun Ni, Xinyu Zhou, He Wen, and Yuheng Zou. Dorefa-net: Training low bitwidth convolutional neural networks with low bitwidth gradients. *arXiv preprint arXiv:1606.06160*, 2016.